

- LENSELINK, W. (1988). PFW-Amersfoort, The Netherlands. Private communication.
- LE PAGE, Y. (1987). *J. Appl. Cryst.* **20**, 264–269.
- NARVAEZ, J. N., LAVINE, B. K. & JURIS, P. C. (1986). *Chem. Senses*, **11**, 145–156.
- OHLOFF, G., WINTER, B. & FEHR, C. (1990). In *Perfumes. Art, Science and Technology*, edited by P. M. MÜLLER & D. LAMPARSKY, pp. 310–325. London & New York: Elsevier Applied Science.
- PESCHAR, R. (1990). SIMPEL88. In *MolEN. Molecular Structure Solution Procedures*, Vol. 3, p. 59. Enraf-Nonius, Delft, The Netherlands.
- SCHENK, H. & HALL, S. (1990). *SIMPEL. Xtal3.0 Reference Manual*, edited by S. R. HALL & J. M. STEWART. Univs. of Western Australia, Australia, and Maryland, USA.
- WALKER, N. & STUART, D. (1983). *Acta Cryst.* **A39**, 158–166.
- WOOD, T. F. (1968). In *Chemistry of the Aromatic Musks*, p. 5. Clifton, New Jersey: Givaudan Corporation.
- YAO, J., ZHENG, C., QIAN, J., HAN, F., GU, Y. & FAN, H. (1985). *SAPI, A Computer Program for Automatic Solution of Crystal Structures from X-ray Data*. Beijing, China: Institute of Physics, Academia Sinica.

Acta Cryst. (1994). **B50**, 737–741

The Charge-Density Distribution in Hexamethylenetetramine at 120 K

BY S. P. KAMPERMANN, J. R. RUBLE AND B. M. CRAVEN*

Department of Crystallography, University of Pittsburgh, Pittsburgh, PA 15260, USA

(Received 14 December 1993; accepted 15 March 1994)

Abstract

The charge-density distribution has been determined from 333 independent X-ray reflections with $\sin\theta/\lambda < 1.47 \text{ \AA}^{-1}$, which were collected with Ag $K\alpha$ radiation. As found in a recent refinement using room-temperature data, full-matrix least squares refinement with a multipole model gives rise to an almost complete correlation between certain octapole deformation terms. This is the worst case example of a problem which will always arise to some degree when applying the multipole model in a noncentrosymmetric space group. In this example, the correlation arises between terms which are predominant for describing the bonding density between atoms of the molecule, thereby causing the deformation charge density to have little meaning. However, the total molecular electrostatic potential and the molecular octapole moment are reliably obtained.

Introduction

The crystal structure of urotropin or hexamethylenetetramine (HMT, $\text{C}_6\text{H}_{12}\text{N}_4$; see Fig. 1) is well known (Dickinson & Raymond, 1923) and has been intensively studied. This highly symmetric molecule crystallizes in a noncentrosymmetric space group with all three atoms in the asymmetric unit (C, N and H) lying in special positions. It is of special interest that the molecular symmetry ($\bar{4}3m$) is fully expressed in the space group $I\bar{4}3m$.

We have measured new low-temperature (120 K) X-ray diffraction data for HMT in order to study the charge-density distribution. New neutron diffraction

data have also been measured at six temperatures (15, 50, 80, 120, 160 and 200 K) in a parallel study of neutron extinction and the nuclear thermal vibrations in HMT (Kampermann, Sabine, Craven & McMullan, 1994).

Terpstra, Craven & Stewart (1993) carried out multipole least-squares refinements for HMT using the pseudoatom model of Stewart (1976) and the room-temperature X-ray data of Stevens & Hope (1975). They found that the octapole deformation terms o_4 for C and N atoms are almost completely correlated in the least-squares refinement. The effect is crucial for a detailed study of the deformation charge density, because the o_4 term largely describes

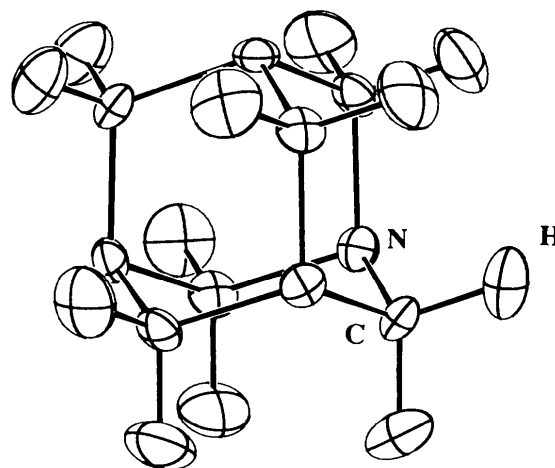


Fig. 1. Molecular structure for HMT (120 K) with harmonic m.s. displacements represented as thermal ellipsoids at the 50% probability level (Johnson, 1976).

* Author to whom correspondence should be addressed.

the bonding density for C and N atoms. A further difficulty was encountered. Although the X-ray data of Stevens & Hope (1975) were considered to be very accurate, it appeared that the large nuclear m.s. displacements in HMT at room temperature have an adverse effect on the deconvolution of the charge-density distribution from the thermal vibrations. Our low-temperature study was undertaken in order to determine the charge-density distribution under more favorable conditions.

We have learned that low-temperature high-resolution X-ray data for HMT have also been measured by Dauter, Grochowski & Serda (private communication). Since these data were collected using Ag $K\alpha$ radiation and an area detector, whereas ours were collected using Ag $K\alpha$ radiation and a conventional diffractometer, there will be interest in a comparison of the two studies.

Experimental

Crystals of HMT were grown from a chloroform solution by slow evaporation. The crystals were rhombic dodecahedra showing the form $\{110\}$. A crystal 0.4 mm in diameter was selected for diffraction measurements. The crystal was mounted on a glass fiber with the reciprocal lattice point 514 close to the φ -axis of the Enraf-Nonius CAD-4 diffractometer. The X-radiation was graphite-monochromatized Ag $K\alpha$ ($\lambda = 0.5608 \text{ \AA}$). The diffractometer was in a sealed box with dried air blown into the box to prevent icing on the crystal. The temperature of the crystal was lowered using a cold stream of nitrogen gas until the cell dimension $a_o = 6.956(3) \text{ \AA}$ was in good agreement with the value $a_o = 6.955(1) \text{ \AA}$ obtained earlier by neutron diffraction at 120 K (Kampermann, Sabine, Craven & McMullen, 1994). The temperature throughout the data collection was maintained at $\pm 1 \text{ K}$ with monitoring by a thermocouple in the cold stream *ca* 8 mm upstream from the crystal. X-ray intensities were measured by $\theta/2\theta$ scans with a speed $0.87\text{--}2.0 \text{ min}^{-1}$. The intensities of three standard reflections ($2\bar{6}2$, $6\bar{2}\bar{2}$, 226) were monitored every 6000 s. Variations up to 7% of the maximum value were observed. The data were analysed using the computer programs of Blessing (1989, and references therein). The intensities were internally scaled, taking into account the variation in the monitor reflections with time. Integrated intensities were obtained from the scan profiles using the method of Lehmann & Larsen (1974). An absorption correction ($\mu = 0.056^\circ \text{ mm}^{-1}$) was applied (Busing & Levy, 1957), which gave correction factors from 1.028 to 1.034. From this calculation the crystal mean path length was also provided (0.236–0.298 mm).

A total of 1549 reflections were collected for one full octant in reciprocal space, comprising all those with $\sin\theta/\lambda < 1.26 \text{ \AA}^{-1}$. Selected strong reflections ($E_{\text{calc}} > 2.0$) were also measured for 89 reflections with $\sin\theta/\lambda = < 1.47 \text{ \AA}^{-1}$, giving a total of 1683. After averaging, 333 independent reflections were obtained with $R_{\text{int}}(F_o^2) = 0.03$.

Structure refinement

The neutron diffraction results for 120 K (Kampermann, Sabine, Craven & McMullen, 1994; see our Table 1) were taken as a starting point for the X-ray refinement. The atomic scattering curves for the Hartree-Fock K-shell of C and N were taken from Cromer & Waber (1974). Radial scattering factors for the spherical component of the C and N Hartree-Fock L-shell charge densities were constructed from a linear combination of Slater-type wavefunctions, as given by Clementi & Roetti (1974). For C and N, κ -parameters were introduced to allow for expansion/contraction of the valence shell (Coppens *et al.*, 1979). The inner K-shells were assigned fixed populations of 2 electrons both for C and N, whereas the number of valence-shell electrons was unconstrained. The radial scattering factor for H as well as the multipole functions for C, N and H were obtained from single Slater-type density functions with standard values for the radial exponents [$\alpha = 6.42, 7.37$ and 4.69 \AA^{-1} for C, N and H (Hehre, Stewart & Pople, 1969)]. The least-squares refinement involved 24 variables, including the overall scale factor applied to the K-shell scattering, $\kappa(\text{C})$, $\kappa(\text{N})$, positional and anisotropic displacement parameters for C and N and all symmetry-allowed electron population parameters in the multipole expansion up to octapoles for C and N and up to dipoles for H. For H, fixed values from neutron diffraction were assumed for the positional and anisotropic m.s. displacement parameters, as well as the third-order anharmonic thermal parameters as defined in the Gram-Charlier formalism (Table 1). Extinction corrections were found to be unnecessary.

The full-matrix least squares refinement included all 333 independent reflections and was carried out with the program *POP* (Craven, Weber, He & Klooster, 1993). The function $\sum w\Delta^2$ was minimized, where $\Delta = |F_o^2| - |F_c^2|$, and $w = \sigma^{-2}(F_o^2)$ with $\sigma^2(F_o^2) = \sigma_{\text{cs}} + (0.02F_o^2)^2$, where σ_{cs} is the variance due to counting statistics. Refinement gave $wR(F^2) = 0.038$, $R(F^2) = 0.023$ and $S = 0.92$. The final values for the refined parameters are given in Table 2, column (a). When the total number of electrons obtained in the refinement was scaled to give an electrically neutral molecule, there were 20.20 K-shell and 55.80 valence-shell electrons, as compared with ideal values of 20 and 56. The p_v -values listed in

Table 1. Nuclear parameters at 120 K

Atoms in the asymmetric unit are as defined by Terpstra, Craven & Stewart (1993) and nuclear parameters are from Kampermann, Sabine, Craven & McMullan (1994). The thermal displacement factor is given by $T = \exp[-2\pi^2 \sum_{j,k} h_j h_k a_j^* a_k^* U^{jk}] - [1 - \frac{1}{3}\pi^3 i \sum_{j,k,l} h_j h_k h_l a_j^* a_k^* a_l^* C^{jkl}]$, where U^{jk} is in units of $\text{\AA}^2 \times 10^4$ and C^{jkl} is in $\text{\AA}^3 \times 10^5$. For H, $C^{111} = 0$ (4), $C^{222} = -C^{333} = 10$ (4), $C^{112} = -C^{113} = -2$ (2), $C^{122} = C^{133} = -2$ (2), $C^{223} = -C^{233} = 0$ (2) and $C^{123} = 2$ (3). For C and N, all $C^{jkl} = 0$.

| | C | N | H |
|----------|------------|------------|-------------|
| <i>x</i> | 0.2414 (1) | 0.1241 (2) | 0.3315 (4) |
| <i>y</i> | 0 | 0.1241 | -0.0913 (4) |
| <i>z</i> | 0 | 0.1241 | 0.0913 |
| U^{11} | 91 (3) | 158 (2) | 246 (6) |
| U^{22} | 220 | 158 | 461 (6) |
| U^{33} | 220 (2) | 158 | 461 |
| U^{12} | 0 | -37 (1) | 96 (5) |
| U^{13} | 0 | -37 | 96 |
| U^{23} | 2 (3) | -37 | 38 (6) |

Table 2. Atomic parameters from X-ray refinement

The values of U^{ij} ($\text{\AA}^2 \times 10^4$) are as defined in Table 1. Population parameters are for deformation terms as defined by Epstein, Ruble & Craven (1982). The columns are: (a) refinement without constraint on the deformation term o_4 ; (b) refinement with constraint on the deformation term o_4 for C, (c) as in (b), except for the data at 298 K (Terpstra, Craven & Stewart, 1993).

| | 120 K | | 298 K |
|----------|--------------|-------------|--------------|
| | (a) | (b) | (c) |
| C | | | |
| κ | 1.01 (1) | 1.02 (2) | - |
| <i>x</i> | 0.24152 (8) | 0.24153 (8) | 0.23810 (5) |
| U^{11} | 101 (2) | 101 (2) | 259 (4) |
| U^{33} | 234 (2) | 233 (2) | 651 (6) |
| U^{23} | -2 (3) | -3 (3) | 5 (8) |
| p_r | 4.02 (10) | 3.95 (10) | 3.97 (8) |
| d_1 | 0.62 (19) | 0.60 (19) | -0.07 (24) |
| q_1 | 0.16 (13) | 0.13 (13) | 1.00 (23) |
| q_4 | -0.20 (31) | -0.16 (32) | -1.51 (50) |
| o_1 | 0.60 (25) | 0.70 (24) | 1.35 (23) |
| o_4 | -4.98 (1.10) | [-2.58] | [-2.36] |
| N | | | |
| κ | 1.010 (9) | 1.012 (9) | |
| <i>x</i> | 0.1243 (2) | 0.1243 (2) | 0.12256 (13) |
| U^{11} | 172 (1) | 172 (1) | 477 (4) |
| U^{12} | -32 (1) | -32 (1) | -107 (3) |
| p_r | 5.14 (9) | 5.19 (9) | 4.99 (12) |
| d_1 | 0.30 (43) | 0.19 (38) | -0.25 (56) |
| q_2 | 0.33 (42) | 0.37 (43) | 0.19 (65) |
| o_1 | 0.43 (40) | 0.42 (38) | 0.93 (49) |
| o_4 | 0.83 (1.12) | 3.25 (25) | 2.85 (28) |
| H | | | |
| p_r | 0.94 (2) | 0.96 (2) | 1.02 (3) |
| d_1 | -1.16 (13) | -1.23 (13) | -1.26 (20) |
| d_2 | 1.06 (19) | 1.06 (19) | 0.29 (28) |

Table 2 are scaled to give a total of 56 valence-shell electrons.

It was found that the least-squares correlation between the octapole population parameters o_4 for C and N was almost the same (0.98 at 120 K) as at room temperature [0.97 (Terpstra, Craven & Stewart, 1993)]. The correlation arises because the o_4 terms affect primarily the phase rather than the magnitude of the resulting structure factor. We fol-

lowed the procedure of Terpstra, Craven & Stewart (1993) by carrying out an additional refinement with the population o_4 for C fixed at -2.5 (becoming -2.58 after rescaling), this being similar to the value obtained in earlier studies involving tetrahedrally bonded carbon (Craven & Weber, 1983; Swaminathan & Craven, 1984). The second refinement gave final $wR(F^2) = 0.038$, $R(F^2) = 0.021$ and $s = 0.94$. The results are given in Table 2, column (b). As expected, there were no significant changes in the parameters except for the octapole terms o_4 .

In both refinements, $\kappa(C)$ and $\kappa(N)$ are slightly greater than 1.0, indicating a slight contraction of the valence density compared with isolated Hartree-Fock atoms. The atomic m.s. displacements (Table 2) are systematically almost 10% larger than the corresponding values from neutron diffraction (Table 1), indicating that, if classical theory applies, the true temperature for X-ray data collection may have been about 130 K. The thermal expansion $\Delta a_0/\Delta T$, as obtained from neutron diffraction (Kampermann, Sabine, Craven & McMullan, 1994), indicates that if the true temperature were 130 K, the cell dimension a_0 would increase by 0.004 \AA (1.3σ in the X-ray measurement). The C-N bond length is 1.469 (2) \AA and the angles C-N-C and N-C-N are 107.88 (9) and 112.58 (8) $^\circ$, respectively, in good agreement with the corresponding values from neutron diffraction at 120 K.*

Discussion

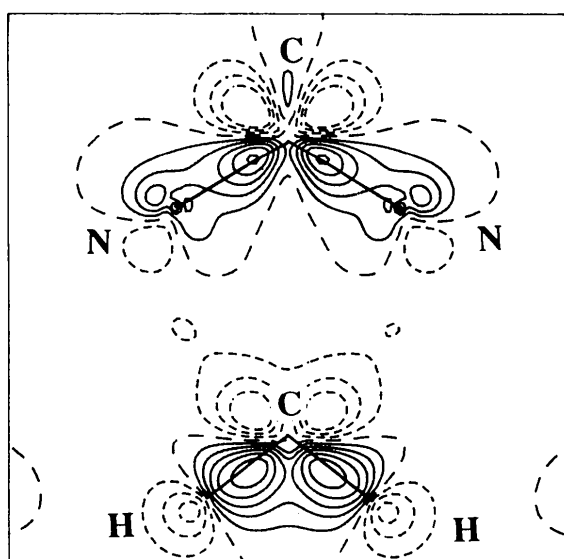
In Fig. 2 we show the deformation charge density for a static arrangement of atoms. These maps are constructed by summing the electron-density deformation terms obtained from the pseudoatom model. The notable difference between the maps [Figs. 2(a) and 2(b)] comes chiefly from the difference in values for o_4 in the constrained and unconstrained refinements. A comparison of Fig. 2 with corresponding maps derived from the room-temperature data (Figs. 4 and 5 from Terpstra, Craven & Stewart, 1993) shows some enhancement of the density in the lone-pair region of the N atoms in Fig. 2. However, the almost complete correlation between o_4 parameters introduces an uncertainty which greatly reduces the value of all these maps. As pointed out by Terpstra, Craven & Stewart (1993), the structure of HMT presents the worst case example of a general problem which must be recognized whenever the multipole model is applied in a structure with a noncentrosymmetric space group.

* A list of reflection data has been deposited with the IUCr (Reference: BK0007). Copies may be obtained through The Managing Editor, International Union of Crystallography, 5 Abbey Square, Chester CH1 2HU, England.

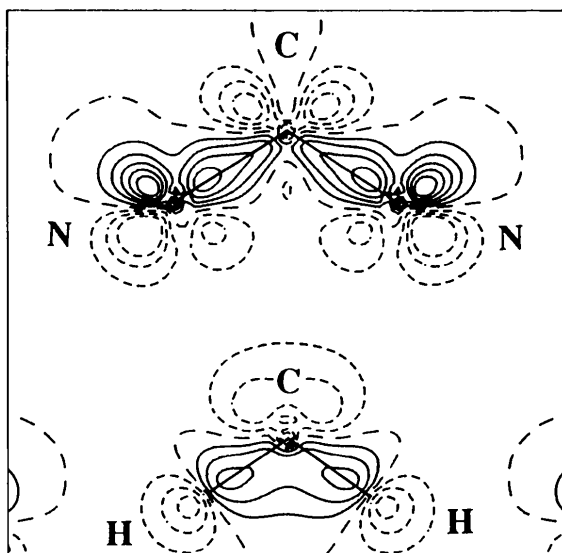
Nevertheless, even for HMT a charge-density study is useful for deriving other electrostatic properties less sensitive to the effects of the o_4 correlations. In Fig. 3 it can be seen that the total electrostatic potential for a molecule removed from the crystal is almost unaffected by the o_4 correlations, except for differences in the electronegativity within the central cage region. As illustrated by Stewart & Craven (1993) in the case of γ -aminobutyric acid, the higher

multipoles have only a short range effect on the potential. The contribution of the octapoles decreases as $1/r^5$, so that their effect is negligible at distances $r > 2.5 \text{ \AA}$ from the atomic nuclei. In Fig. 3, the feature in the molecular environment which is of greatest chemical significance is the electronegative region near each N atom.

Because of the tetrahedral point symmetry of HMT, the first nonzero molecular moment is the

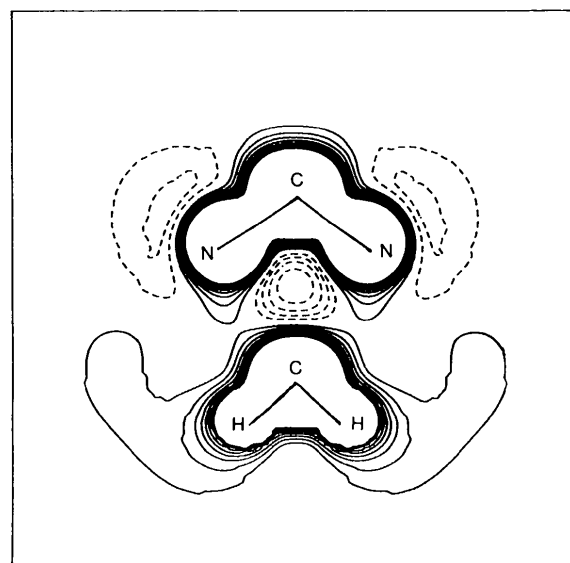


(a)

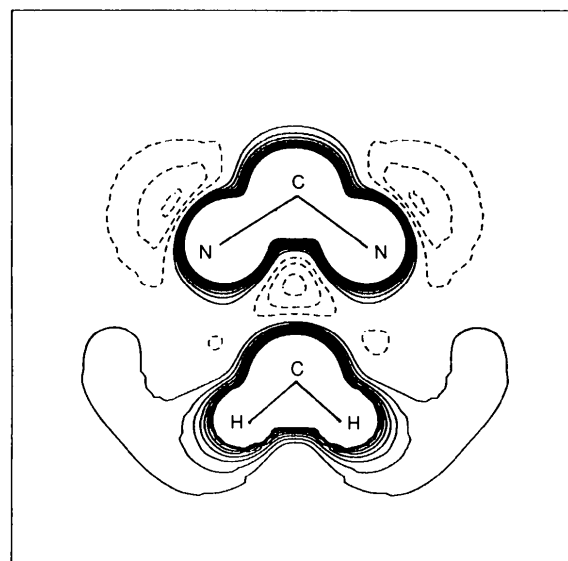


(b)

Fig. 2. Static deformation density map in the plane through N—C—N (top) and H—C—H (bottom) of the same molecule. Contours are at intervals of 0.1 e \AA^{-3} . (a) Derived from the refinement without constraint on the deformation term o_4 , (b) derived from the refinement with such a constraint.



(a)



(b)

Fig. 3. Total electrostatic potential for a complete HMT molecule removed from the crystal structure. Contours are at intervals of 0.05 e \AA^{-1} with solid and dashed contours for regions of electropositivity and negativity, respectively. (a) Derived from the refinement without constraint on the deformation term o_4 , (b) derived from the refinement with such a constraint.

octapole. The experimental value for the octapole moment of HMT, derived including all multipole terms up to octapole, is $\langle xyz \rangle = +1.4(2)|e|\text{\AA}^3$, using population parameters obtained without constraint on the o_4 parameters. The corresponding value from Terpstra, Craven & Stewart (1993) is $\langle xyz \rangle = +1.0(3)|e|\text{\AA}^3$. When the o_4 parameters are constrained, the value derived from Table 2, column (b), is $1.9(2)|e|\text{\AA}^3$. Corresponding octapole moments as defined by Buckingham (1970) are $\Omega = \frac{2}{3}\langle xyz \rangle = -5.5(7)$, $-4.0(14)$ and $-7.6(6) \times 10^{-49} \text{ C m}^3$, respectively. Although an increasing number of molecular dipole and quadrupole moments is being reported (Spackman, 1992), HMT appears to provide the first example of a molecular octapole moment determined from Bragg diffraction data.

This work was supported by grants GM-31593 and HL-20350 from the US National Institutes of Health. We are grateful to Mrs Joan Klinger for technical assistance.

References

- BLESSING, R. H. (1989). *J. Appl. Cryst.* **22**, 396–397.
 BUCKINGHAM, A. D. (1970). In *Physical Chemistry: An Advanced Treatise*, Vol IV, edited by H. EYRING, D. HENDERSON & W. JOST. New York: Academic Press.
 BUSING, W. R. & LEVY, H. A. (1957). *Acta Cryst.* **10**, 180–182.
 CLEMENTI, C. & ROETTI, C. (1974). *Atomic Data and Nuclear Data Tables*, Vol. 14, pp. 177–178. New York: Academic Press.
 COPPENS, P., GURU ROW, T. N., LEUNG, P., STEVENS, E. D., BECKER, P. J. & YANG, Y. W. (1979). *Acta Cryst.* **A35**, 63–72.
 CRAVEN, B. M. & WEBER, H. P. (1983). *Acta Cryst.* **B39**, 743–748.
 CRAVEN, B. M., WEBER, H. P., HE, X. M. & KLOOSTER, W. (1993). *The POP Procedure, Computer Programs to Derive Electrostatic Properties from Bragg Reflections*. Technical Report, Department of Crystallography, Univ. of Pittsburgh, PA, USA.
 CROMER, D. T. & WABER, J. T. (1974). *International Tables for X-ray Crystallography*, Vol. IV, pp. 71–147. Birmingham: Kynoch Press. (Present distributor Kluwer Academic Publishers, Dordrecht.)
 DICKINSON, R. G. & RAYMOND, A. L. (1923). *J. Am. Chem. Soc.* **45**, 22–29.
 EPSTEIN, J., RUBLE, J. R. & CRAVEN, B. M. (1982). *Acta Cryst.* **B38**, 140–149.
 HEHRE, W. J., STEWART, R. F. & POPLE, J. A. (1969). *J. Chem. Phys.* **51**, 2657–2664.
 JOHNSON, C. K. (1976). *ORTEPII*. Report ORNL-5138. Oak Ridge National Laboratory, Tennessee, USA.
 KAMPERMANN, S. P., SABINE, T. M., CRAVEN, B. M. & McMULLAN, R. K. (1994). In preparation.
 LEHMANN, M. S. & LARSEN, F. K. (1974). *Acta Cryst.* **A30**, 580–584.
 SPACKMAN, M. A. (1992). *Chem. Rev.* **92**, 1769–1797.
 STEVENS, E. D. & HOPE, H. (1975). *Acta Cryst.* **A31**, 494–498.
 STEWART, R. F. (1976). *Acta Cryst.* **A32**, 565–574.
 STEWART, R. F. & CRAVEN, B. M. (1993). *Biophys. J.* **65**, 998–1005.
 SWAMINATHAN, S. & CRAVEN, B. M. (1984). *Acta Cryst.* **B40**, 511–518.
 TERPSTRA, M., CRAVEN, B. M. & STEWART, R. F. (1993). *Acta Cryst.* **A49**, 685–692.

Acta Cryst. (1994). **B50**, 741–746

Electrocrystallization, Crystal Structure and Physical Properties of Hexaperylene Hexafluorophosphate, $(\text{C}_{20}\text{H}_{12})_6^+ \text{PF}_6^-$

BY WERNER F. KUHS AND GÜNTER MATTERN

Institut für Kristallographie, Universität Karlsruhe, D-76128 Karlsruhe, Germany

WOLFGANG BRÜTTING

Experimentalphysik II, Universität Bayreuth, D-95440 Bayreuth, Germany

AND HEDWIG DRAGAN, MICHAEL BURGGRAF, BERND PILAWA AND ELMAR DORMANN

Physikalisches Institut, Universität Karlsruhe (TH), D-76128 Karlsruhe, Germany

(Received 10 January 1994; accepted 13 April 1994)

Abstract

Electrocrystallization and crystal structure are reported for the 6:1 salt of perylene (PE) and hexafluorophosphate. The three-dimensional crystal structure contains PE dimers with very small intra-

dimer and large interdimer separation. Measurements of static magnetic susceptibility and d.c. electrical conductivity characterize $(\text{PE})_6\text{PF}_6$ as an organic semiconductor with comparatively large activation energy and one Curie-like radical spin per formula unit.